An in-situ FTIR spectroscopic study of the electrochemical oxidation of ethanol at a Pb-modified polycrystalline Pt electrode immersed in aqueous KOH.

P. A. Christensen, S. W. M. Jones and A. Hamnett

School of Chemical Engineering and Advanced Materials, Bedson Bulding, Newcastle University, Newcastle upon Tyne, NE1 7RU, England, UK.

Keywords: FTIR, alkaline, Pt, Pb, oxidation, thin-layer, carbonate.

ABSTRACT

A study of the mechanism of ethanol oxidation in alkaline solution on a platinum electrode modified with an irreversibly-deposited layer of lead has been carried out using *in situ* FTIR spectroscopy. This study provides support for the suggestion that the adsorption mechanism of ethanol is substantially modified in the presence of Pb, with a carbon-bonded intermediate being favoured leading to facile scission of the C-C bond in ethanol. We have found that the formation of carbonate takes place at potentials close to the thermodynamic value. At higher potentials, when Pb is lost to solution, the mechanism of oxidation of ethanol reverts to that found on a normal polycrystalline Pt surface, with the primary product being acetate.

1. INTRODUCTION

Ethanol is of interest as a renewable energy source as it can be produced in large quantities from sugar-containing feedstocks, including waste biomass, and it is widely available[1][2]. There has been particular interest in using ethanol in low temperature, direct alcohol fuel cells, employing acidic, Polymer Electrolyte Membranes (PEM's) such as Nafion. However, the platinum and Pt-based anodes in such devices are poor electrocatalysts for ethanol oxidation in acid, since the reaction is inhibited by strongly adsorbed fragments such as C≡O. In addition, C-C bond cleavage is inefficient, and the major products of the oxidation of ethanol at the anode of such fuel cells are acetaldehyde and acetic acid (see [3] and references therein), and these release only 2 and 4 electrons, respectively, of the 12 available for complete oxidation of ethanol, representing a poor fraction of the full 8 kWh kg^{-1} specific energy density potentially available[4].

This remains a major challenge to fuel-cell designers, and, as a result, there has been a resurrection of interest in recent years in the use of alkaline fuel cells, because both alcohol oxidation and oxygen reduction are more facile under alkaline conditions than acid[5]. It has been suggested that the enhanced kinetics in alkaline solution may arise from the readier availability of 'active oxygen' in the form of reversibly adsorbed OH[6], and it is certainly true that there is a wider range of moderately active catalysts available: eg. Pd is inactive towards ethanol oxidation under acid conditions, but is more active than Pt in alkali[7]. However, whilst the selective oxidation of ethanol to CO_3^{2-} at Pt in alkaline media has been reported at high overpotentials ([8] and references therein), the problem of incomplete oxidation at the lower, commercially significant, potentials still remains. This poor selectivity for ethanol oxidation to carbonate at Pt has been attributed to[8] the adsorption of the ethanol molecule via the O atom on the C_1 carbon; the removal of the first two electrons from the adsorbate then generates acetaldehyde, CH_3CHO, which is able to desorb (see scheme 1) as such, but can also itself be oxidised in a second two-electron step to acetate, which in turn can be displaced from the surface by the ethanol in solution. Work in Newcastle on methanol[9], formate[10] and ethanol[11] oxidation supports this postulate in terms of oxidation in alkaline media, with clear evidence of adsorption through O rather than through C, and with evidence that it is adsorption through the the latter of which is necessary for C-C cleavage.

Recently, He and co-workers[8] reported a marked enhancement in the cleavage of the C-C bond of ethanol at Pt nanocrystals supported on carbon in 0.25M KOH in the presence of $Pb(OAc)_4$ as co-catalyst. The extent of this enhancement appears to depend critically on the conditions of the experiment, possibly owing to the hydrolysis of the lead tetra-acetate itself to PbO_3^{2-} in alkaline solution; but all experiments show an enhancement. The authors speculated that the mechanism shown in scheme 1 may be operating; in this, the presence of upd Pb on the Pt surface and Pb(IV) in solution could facilitate the formation of a C-C bonded intermediate that could, in turn, be oxidised completely to carbonate. Complete oxidation of ethanol was postulated over the potential range which the upd Pb (deposited at potentials below 0.4V vs RHE) was oxidised to adsorbed $HPbO_2^-$ at ca. 0.46V to 0.77V vs RHE, the latter providing the necessary 'active oxygen'. Without the solution Pb(IV), the activity was observed to decline and the authors postulated that this was due to poisoning by adsorbed CO or other intermediates from the chemisorption of ethanol, and that the Pb(IV) solution species plays a major role in activating the C-C bond in conjunction with the Pb on the surface. An alternative possible explanation is that adsorbed CO displaces the Pb as was observed in acidic solution for Pb adlayers on Pt(100) and Pt(111)[12][13].

The postulated enhancement of C-C bond breaking at Pt in the presence of Pb by He et al. is supported only by the DEMS data at 0.67V and 0.77V, and the actual potential range over which this occurs was not verified by experiment and no other molecular, analytical data were presented. In addition, the authors stated that the DEMS experiments were problematic, with no multi-electron products (eg. acetate) detected below 700 mV. In order to provide molecular information as a function of potential, this paper presents an initial, in-situ FTIR spectroscopic study of the effect of the presence of Pb on the oxidation of ethanol at polycrystalline Pt in 0.25M KOH. For this study, a polycrystalline Pt electrode was employed with Pb pre-deposited, to avoid optical problems due to deposition taking place during spectral data collection. No lead solution species were thus present at the commencement of the FTIR experiments discussed below.

2. EXPERIMENTAL

The electrolyte solutions were prepared using Millipore water (18.2 MΩ cm). Aqueous 0.25 M KOH (Aldrich SigmaUltra >85% KOH basis) was employed as supporting electrolyte. Ethanol (Aldrich spectrophotometric grade >99.9% ACS) was used as received. Nitrogen gas from a cryogenic boil-off was employed to de-aerate the solutions and to maintain an air-free atmosphere over the electrolyte during the measurements. All potentials were measured *vs*. a Hg/HgO (Mercury Mercury Oxide, MMO Sentek) electrode in aqueous 0.1M NaOH, which was calibrated using a Pt electrode against a Reversible Hydrogen Electrode in this solution; the results are all quoted with respect to RHE. The polycrystalline Pt (pc-Pt) electrode was 'top hat' shaped with an area of 0.64 cm^2 polished and exposed to the electrolyte[1-3].

The electrode was polished with 0.015 μm alumina (BDH), washed thoroughly with Millipore water and then immersed in Millipore water in an ultrasonic bath for several minutes prior to transfer into the spectro-electrochemical cell. The Pb was removed from the Pt electrode by immersing the latter in aqua regia and washing with Millipore water, these repeated several times. The spectroelectrochemical cell has been described in detail elsewhere[4]. The cell was mounted vertically on the lid of the sample compartment of the spectrometer via an aluminium plate, and was designed to allow electrolyte exchange under potential control. The cell was jacketed to allow careful control of the temperature of the electrolyte in the body of the cell, which was facilitated by circulating heating or cooling fluid through the hollow aluminium mounting plate using a Grant cooling/heating unit.

Lead was deposited on the pc-Pt electrode as follows: 1mM Pb(IV) acetate (Aldrich, 95%) + 0.25M KOH was admitted into the IR cell and the potential held at +0.10V vs RHE for 15 minutes, after

which half the electrolyte was replaced by 0.25M KOH (still under potential control) eight times, reducing the Pb(IV) acetate concentration in solution to $< 10^{-6}$ M. Ethanol was then added to the electrolyte, via a pipette, to a final concentration of 1M, and the solution agitated thoroughly to ensure effective mixing. Based on the seminal papers by Clavilier et al[14] and Feliu and co-workers[15] on Pb deposition on well-defined Pt surfaces in acid and alkaline solution, the electrochemical response of the Pb shows that the metal is irreversibly adsorbed on the Pt, rather than having undergone underpotential deposition (upd).

The electrode was then pushed against the cell window and a reference spectrum (S_R, 100 co-added and averaged scans at 8 cm^{-1} resolution, *ca*. 35 s per scanset) collected immediately, after which a second spectrum was collected at 0.10V before the potential of the Pt electrode was stepped up, with further spectra taken at each step. The spectra below are presented as:

$$\text{Absorbance, } A = \text{Log}_{10}(S_S/S_R) \quad (1)$$

This data manipulation results in difference spectra in which peaks pointing up, to +(Absorbance), arise from the gain of absorbing species in S_S with respect to S_R, and peaks pointing down, to -(Absorbance), to the loss of absorbing species. Spectra were collected up to 1.35V, but the potential range of primary interest in the discussion below was that employed in the work of He et al.[8], ie. ca. 0.10V to 1.00V.

In the ethanol chemisorption experiments, lead was deposited as described above. After removal of the $Pb(OAc)_4$ from the electrolyte by dilution, ethanol was added to a concentration of 1M and left to chemisorb (at +0.15V) for 10 minutes after which it was removed from solution by dilution, the electrode pressed against the cell window and data collection started.

The optical pathlength was estimated from the 1640 cm^{-1} H-O-H scissor band in the single beam reference spectrum; this calculation and the measures taken to ensure consistent pathlength of *ca*. 3 – 4 μm are given in detail in our previous papers and/or the references therein[1-3].

Cyclic voltammetry experiments were carried out in a standard, 3-electrode cell (electrolyte volume 30 cm^3) using a 1 cm^2 Pt mesh working electrode (50% open area), 2 cm^2 Pt/Ti mesh counter electrode and a MMO reference electrode.

3. RESULTS AND DISCUSSION

Voltammetry

Figure 1(a) shows cyclic voltammograms of the Pt mesh electrode with and without the Pb layer in 0.25M KOH. The CV in the presence of the Pb is very similar to that presented by He et al[8], allowing for the different morphologies of the Pt electrodes, and the peak potentials of the oxide stripping features (and the hydride features in the absence of Pb) were employed to confirm the conversion between the MMO reference electrode employed and the RHE. The deposition of Pb suppresses the adsorption of hydrogen completely (on the timescale of the experiment), and the anodic region of the voltammogram is enhanced due to the oxidation of Pb initially to adsorbed oxo-hydroxide species of lead[14] and to $HPbO_2^-$ in solution, a process that commences at about 0.46V[16], but which is very irreversible. Further oxidation continues both of the lead layer and the underlying Pt in the region 0.70 - 1.20V vs. RHE, and certainly at the higher potentials in this range, oxidation of the lead to Pb(IV) is possible.

The thermodynamic potential for oxidation of $HPbO_2^-$ to PbO_3^{2-} at pH 13.3 is given by Carr and Hampson[16] as E^0 (NHE) = 1.40 - 0.0886pH; converting this to our RHE gives 1.00V, and this would therefore account for the obvious rise in current at the most positive potentials in figure 1 compared to Pt itself. However, He et al. suggest that the current above 0.80V could be due to this oxidation process, but this seems improbable on the basis of Carr and Hampson's article. Furthermore, oxidation of Pb(II) to $Pb(OAc)_4$ is known to occur at about 1.40V vs. RHE in dilute acetic acid[17], and in alkaline solution, the E^0 value vs. RHE will be given approximately as 2.20 – 0.0886pH ≈ 1.00V, which does account for the increasing current beyond 1.00 V in fig. 1(a), as compared to Pt.

The considerable irreversibility in the anodic current associated with the oxidation of the lead layer is interesting: lead adsorbed on single-crystal Pt surfaces is known to attain essentially complete coverage on all low index faces[14][18], a result entirely consistent with the disappearance of the hydride structure. However, polycrystalline and nanocrystalline Pt will have micro-regions of well-defined surface structure interspersed with less regular arrangements of Pt atoms at the interfaces between these regions: the lead will probably adsorb to lower coverage in these interfacial areas of the surface, leading to a surface structure at low potentials consisting of well-defined lead islands and gaps between these islands where there is a lower lead coverage. Oxidation of such a structure will then begin at the edges of the island superstructures, presumably initially by formation of adsorbed Pb-OH, and will progress at different rates on different Pt surface structures, accounting for the obvious broadness of the oxidation process. In addition, the oxidation may well proceed in

two stages on each surface region, the first oxidation creating a still adsorbed oxo-hydroxide Pb surface and the second step being further oxidation and removal of this as $HPbO_2^-$. Further oxidation of this as a solution species to $Pb(OAc)_4$ and PbO_3^{2-} in solution then taking place at more positive potentials.

Figure 1(b) shows the voltammograms in the presence of 1 M ethanol. In agreement with the work of He and co-workers, there is a significant enhancement in the currents of both the peak in the anodic sweep and the anodic (auto-oxidation) peak on the return (cathodic) sweep due to oxidation of the ethanol at the freshly-exposed Pt following oxide stripping. The former is enhanced by a factor of > 4 in the presence of Pb (compared to the threefold enhancement observed by He et al). However, there are also some differences: thus, He et al observe a marked shift in onset potential of 150 mV to more negative potentials, such a shift is not evident in fig. 1(b) (but is in the IR data, see below). Furthermore, He and co-workers observed that the auto-oxidation peak observed as the Pt oxide starts to strip in the cathodic sweep was very sharp and twice that of the anodic peak current; in contrast, as can be seen in fig. 1(b), both features are broad, the auto-oxidation feature is lower than the anodic peak and clearly comprises two distinct processes, at 0.74V and 0.66V. It is likely that these differences probably reflect the difference in morphology between the polycrystalline Pt electrode employed in this work and the nanoparticulate Pt employed by He et al.

Infrared data

Figure 2 shows the current/potential response observed during FTIR experiments with (i) and without (ii) Pb in which the potential of the reflective Pt working electrode was stepped up from 0.10V, spectra collected at each step and normalised to the reference taken at 0.10V. The spectra collected from the Pb-modified electrode are shown in in figs. 3(a) – (c). The spectra in fig. 3(a) show: the growth of water gain features near 3335 cm^{-1} and 1647 cm^{-1}, the loss of OH^- (broad bands near 2700 and 1875 cm^{-1}[9 - 11]), the gain of a band due to bridge-bonded CO (CO_B) at 1862 cm^{-1} [19][20], the gain of a band near 1395 cm^{-1} with a small gain feature at ca. 1300 cm^{-1}. The CO_B and 1300 cm^{-1} features may be seen more clearly in fig. 3(b) which shows only the spectrum collected at 0.25V. The 1395 cm^{-1} band was unequivocally assigned to solution carbonate by adding Na_2CO_3 dissolved in 0.1M KOH into the FTIR cell containing 0.1M KOH and following the diffusion of the CO_3^{2-} ions into the thin layer with time. The spectrum of CO_3^{2-} so obtained is shown in fig. 4; also shown is the spectrum collected at 0.45V in fig. 3(a) for comparison. Figure 3(c) shows the spectra collected at 0.55V to 0.85V in the experiment depicted in fig. 3(a).

The CO_B feature appears at 0.10V, increases in intensity to 0.35V after which it decreases and is absent at 0.45V, see fig. 5 which shows plots of the intensities of the various features observed in fig. 3(a) as a function of potential. The 1300 cm^{-1} feature appears at the same potential, its intensity increases to a maximum at 0.25V before decreasing. On the basis of the potential dependence of the intensities of the latter feature and the carbonate band, it is clear that the two features are associated with different processes; the 1300 cm^{-1} feature may tentatively be attributed to HCO_3^- associated with water molecules in the Inner Helmholtz Plane[21 - 23]. The frequency of this feature is postulated as being strongly dependent upon the electrolyte[22] and has been observed at 1319 cm^{-1} in alkaline electrolyte[23]. The presence of CO_B (as opposed to linearly-adsorbed C≡O) is noteworthy as CO in bridging and threefold sites on Pt is generally believed to be a poison, blocking the active sites and reducing catalytic activity[24]. The 1862 cm^{-1} band is only present at low potentials and its potential dependence of the does not appear to suggest it is intermediate in the formation of CO_3^{2-}. Hence, CO_B may only be a product from the initial chemisorptions of ethanol, blocking the surface until a sufficiently high potential is attained for it to be oxidised.

The spectra in fig. 3(c) are dominated by the features due to solution acetate (1554 and 1415 cm^{-1}[3]), with an inflexion to the low wavenumber side of the latter feature. This, and the fact that the 1554 cm^{-1} band appears *less* intense than the 1415 cm^{-1}[11], suggest the continuing growth of the carbonate band. The variation in intensity of the carbonate feature between 0.65V and 0.85V was estimated by increasing the intensity of the 1395 cm^{-1}carbonate band in the spectrum taken at 0.45V by factors sufficient to annul its contribution following subtraction from the spectra taken at these potentials. Thus, it was found that increasing the absorbance of the 1395 cm^{-1} band taken at 0.45V by factors of 1.58, 2.18 and 2 and subtracting the resultant spectra from those collected at 0.65V, 0.75V and 0.85V, respectively, resulted in spectra showing no carbonate features and the 1554 & 1415 cm^{-1} bands of acetate in the correct intensity ratios, see fig. 6. Plots of the 1554 cm^{-1} acetate and 1395 cm^{-1} carbonate bands are plotted as a function of potential in fig. 5, which also shows the corresponding plot of the 1554 cm^{-1} band in the absence of Pb. No carbonate was observed in the latter experiment (nor in our previous work in 0.1M KOH[11]).

Returning to fig. 3(c), it can be seen that, at potentials > 0.45V, ie around the onset of oxidation of the lead layer and the production of acetate (see fig. 5), a relatively sharp peak appears at ca. 3680 cm^{-1} and grows in intensity up to 0.95V, after which it decreases, see figs. 5 and 7. Intriguingly, if the IR of acetate oxidation on Pt alone with no lead is studied, then a similar peak is seen at 3680 cm^{-1} but referenced to the spectrum at 0.10V, this peak is now a *loss* feature (see fig. 8), and a similar loss feature is observed for the oxidation of ethanol on Pt without Pb present (see figs. 9 and

10; fig. 9 is taken from our earlier work in 0.1M KOH[11] and fig. 10 shows a repeat of the experiment in fig. 9 except using 0.25M KOH). The presence of this sharp band at such a high frequency was ascribed in our earlier work to the presence of 'isolated' Pt-OH species, isolated in the sense that they are not part of any extended H-bonded structure. This is well established as an idea in the literature: in the limit, as hydrogen bonding is reduced, we would expect a narrow high-frequency band to reflect an O-H stretch free from hydrogen-bonding[25], and this concept has found application in the study of the IR absorptions of the water of hydration and O-H stretches in ionic crystals[26]. Certain ionic crystals have OH^- ions essentially free from hydrogen bonding, and frequencies as high as 3700 cm^{-1} have been observed, e.g. $Mg(OH)_2$[27].

Physically, 'isolated' O-H, ie adsorbed OH species without extensive hydrogen bonding to water molecules, could arise if, for example, they formed in small islands or domains, or were in some other way 'protected' from H-bonding. Given that acetate adsorbs extensively at lower potentials on Pt in the presence of both ethanol and acetate ions in solution, and that O-O adsorbed acetate will present a relatively hydrophobic outer Helmholtz layer, we can tentatively ascribe this high frequency OH stretch to adsorbed OH occupying single sites in regions where otherwise the dominant adsorbate is acetate itself. Some further support for this comes from the fact that the higher the concentration of KOH used as the supporting electrolyte, the larger this loss feature in the spectra derived from the Pt surfaces without Pb present for both acetate and ethanol oxidation (compare figs. 9 and 10).

However, the 3680 cm^{-1} feature is present as a *gain* when lead is present on the surface. Furthermore, this gain feature grows steadily with potential above the point at which the surface begins to lose Pb. If this band is associated with adsorbed acetate, then its behaviour is understandable: there is evidently very little adsorbed acetate on the Pb-covered surface, and only once the Pb starts to be removed does sufficient co-adsorption of acetate and OH take place.

This then raises a further point: if there is no adsorbed acetate, then conversion of ethanol to acetate at the surface is not taking place at lower potentials. Indeed, it is evident that at low potentials the route taken by the ethanol during oxidation must be quite different from that observed on pure Pt surfaces. Support for this comes not only from the clear evidence for the formation of carbonate at astonishingly low potentials, but also the appearance of a bridged CO species, which we do not see on normal Pt. This bridged CO species vanishes at potentials lower than those associated with the oxidation of the adsorbed Pb, and there is no obvious correlation with the formation of carbonate,

but it may be an intermediate on the route to carbonate, whose coverage is a dynamic balance between formation and removal rates.

We therefore have the following observations: (i) there is little adsorbed acetate on the Pt-Pb surface; (ii) the Pt-Pb surface has a high coverage of Pb at low potentials; (iii) the coverage of Pb on Pt begins to decrease above about 0.45 V; (iv) bridge-bonded CO forms at low potentials on Pt-Pb but disappears above 0.40V; (v) carbonate is observed even at low potentials as a product of the oxidation of ethanol on Pt.

To reconcile these observations, the Pt-Pb can be pictured with the structure discussed above: much of the surface is formed from well-ordered microcrystalline low-index surfaces, but with regions between them where the coverage of the lead is lower. Ethanol does not adsorb on lead itself, so oxidation of ethanol must take place by adsorption on those areas of the surface not covered with Pb. Adsorption must take place either through the O or C_1 atoms of the ethanol; the former would be the normal route on Pt in KOH, and we have postulated[11] that in the absence of solution ethanol, the adsorbed ethoxide can bond through the C_2 carbon giving rise to a cyclic intermediate for which C-C bond cleavage is reasonably facile. However, it is also possible that the small areas of exposed Pt between the Pb islands are appreciably more hydrophobic, and actually favour adsorption through C_1; cyclisation as postulated by He et al. could then take place as shown in figure 1.

It is clear that ethanol is oxidised to carbonate even at 0.10V at the Pb-modified electrode; in fact, two spectra were recorded at 0.10V, one 2 minutes after the first, which clearly showed oxidation taking place even at this low potential, see fig. 11. This is a remarkable result, as the standard potential is close to 0V. Interestingly, Lai and Koper [28] observed adsorbed CO at a Pt/roughened gold anode from ethanol chemisorptions in alkaline solution at ca. 1960 cm^{-1} using SERS at potentials as low as 0.10V vs RHE; thus it appears that the surface of Pt can be engineered either physically (as Lai and Koper did) or chemically (as we have done) to allow the generation of adsorbed ethanol fragments at very low potentials. Whatever the details of the intermediate adsorbate, it is clear that the actual oxidation process is extremely facile once the ethanol is adsorbed, and this suggests the existence of some form of adsorbed OH at very low potentials. This is not an impossibility: Schmidt and co-workers [29] have reported that OH adsorption takes place in the H_{upd} region at Pt in alkaline solution, such that the coverage of these species cannot be determined by simple coulometry. In addition, this OH must be adsorbed on Pt and not on Pb; there is no evidence for the latter at these very low potentials. One possibility is that the OH is actually adsorbed on the Pt adjacent to adsorbed Pb sites, and the picture becomes one of Pb islands on the

surface surrounded by OH_{ads} species. Adsorbed ethanol forming next to such a site would be oxidised easily, and the site could continually recharge, permitting a catalytic cycle to develop.

At higher potentials, the Pb islands start to become oxidised, and also shrink as the Pb is lost to solution as $HPbO_2^-$. As the islands shrink, the Pt surface exposed becomes more and more similar to normal Pt, giving rise to a transition from carbonate to acetate formation. It would appear that only at the lowest potentials, with rather small regions of exposed Pt between Pb islands, is the behaviour such that carbonate is the main product.

Despite the fact that the current passed during the FTIR experiment using the Pb-modified electrode is higher (see figs. 1 & 3), significantly more acetate is produced using the unmodified electrode, see fig. 5, supporting the observation of appreciable carbonate as an additional product in the former experiment. It can be seen from fig. 5 that the intensity of the 1554 cm^{-1} acetate band in the absence of Pb is ca. 2.5x that in its presence, in approximate agreement with the threefold increase in charge required to produce carbonate over acetate

4. CONCLUSIONS

This paper presents a study of the oxidation of ethanol at a Pb-modified, polycrystalline Pt anode in 0.25M KOH. Very surprisingly, we observe significant carbonate formation at very low potentials (ie. 0.10V vs RHE); in order to explain these data, we have postulated a model the essence of which is that carbonate formation takes place at atypical Pt domains between Pb islands. As the Pb is stripped from the surface, the Pt domains become increasingly similar to 'normal' Pt, resulting in increasing acetate formation. If our model is correct, the extent of catalysis is restricted, since only at the particular edges of Pb islands will appropriate conditions exist for oxidation. If we are to develop this catalysis, it will be essential to fabricate a surface in which the formation of Pb islands is carefully controlled so as to leave exposed Pt in regions large enough to act as efficient catalytic centres, but sufficiently small that the highly unusual properties seen in the results presented above can be retained.

AUTHOR INFORMATION

Corresponding author

paul.christensen@ncl.ac.uk

Present address

The School of Chemical Engineering and Advanced Materials, Bedson Building, Newcastle University, Newcastle upon Tyne, NE1 7RU

Notes

The authors declare no competing financial interest.

ACKNOWLEDGEMENTS

We should like to thank the EPSRC for funding under the Hydrogen and Fuel Cells Supergen initiative.

REFERENCES

1. Cremers, C.; Bayer, D;, Kintzel, B.; Joos, M., Krausa, M.; Martin, D., *ECS Trans*., **2009**, 17, 517 – 524.
2. Bayer, D.; Berenger, S.; Joos, M.; Cremers, C. and Tűbke, J., *Int. J. Hydrogen Energy*, **2010**, 35, 12660 – 12667.
3. Shen, S. Y.; Zhao, T. S.; Xu, J. B. and Li, Y. S., *J. Power Sources*, **2010**, 195, 1001 – 1006.
4. Li, M.; Zhou, W. –P.; Marinkovic, N. S.; Sasaki, K. and Adzic, R. R., *Electrochim. Acta*, **2013**, 104, 456 – 461.
5. Shen, S. Y.; Zhao, T. S. and Xu, J. B., *Electrochim*. *Acta*, **2010**, 55, 9179 -9184.
6. Tripković, A. V.; Popović, K. Dj. and Lović, J. D., *Electrochim. Acta*, **2001**, 46, 3163 - 3173.
7. Cui, G.; Song, S.; Shen, P. K.; Kowal, A. and Bianchini, C., *J. Phys. Chem. C*, **2009**, 113, 15639 – 15642.
8. He, Q.; Shyam, B.; Macounova, K.; Krtil, P.; Ramaker, D. and Mukerjee, S., *J. Am. Chem. Soc*. **2012**, 134, 8655 – 8661.
9. Christensen, P. A. and Linares-Moya, D., *J. Phys. Chem. C*, **2009**, 114, 1094−1101.
10. Christensen, P. A.; Hamnett, A. and Linares-Moya, D., *Phys. Chem. Chem. Phys*. **2011**, 13, 11739−11747.
11. Christensen, P. A.; Jones, S. W. M. and Hamnett, A., *J. Phys. Chem. C*, **2012**, 116, 24681−24689.
12. Lucas, C. A.; Marković, N. M.; Grgur, B. N. and Ross, P. N., *Surface Science*, **2000**, 448, 65 – 76.
13. Lucas, C. A.; Marković, N. M. and Ross, P. N., *Surface Science*, **2000**, 448, 77 – 86
14. Clavilier, J.; Orts, J. M.; Feliu, J. M. and Aldaz, A., *J. Electroanal. Chem*., **1993**, 293, 197 – 208
15. Feliu, J. M.; Fernandex-Vega, A.; Orts, J. M. and Aldaz, A., *J. Chim Phys.*, **1991**, 88, 1493 – 1518
16. Carr, J. P. and Hampson, N. A., *Chem. Rev*. **1972**, 72**,** 679 – 703.
17. Berke, A.; Dvořák, V.; Němec, I. and Zýka, J., *J. Electroanal. Chem*. **1962**, 4, 150 – 155.
18. Grgur, B. N.; Marković, N. M. and Ross, P. N. Jr., *Langmuir* **1997**, 13, 6370 – 6374.
19. Zhou, Z-Y.; Wang, Q.; Lin, J-L.; Tian, N. and Sun, S-G., *Electrochimica Acta*, **2010,** 55, 7995 – 7999.
20. Morallón, E.; Vázquez, J. L.; Pérez, J. M. and Aldaz, A., *J. Electroanal. Chem*., **1995**, 380, 47 – 53.
21. Iwasita, T.; Rodes, A. and Pastor, E., *J. Electroanal. Chem*., **1995**, 383, 181 – 189.
22. Iwasita, T.; Nart, F. C.; Rodes, A.; Pastor, E. and Weber, M., *Electrochimica Acta*, **1995**, 40, 53 – 59.

23. Lai, S. C. S.; Kleijn, S. E. F.; Fatma, T. Z.; Öztürk, F. T. Z.; van Rees Vellinga, V. C.; Koning, J.; Rodriguez, P.; Koper, M. T. M., *Catal. Today*., **2010**, 154, 92 − 104.
24. Casado-Rivera, E.; Volpe, D. J.; Alden, L.; Lind, C.; Downie, C.; Vázquez-Alvarez,T.; Angelo, A. C. D.; DiSalvo, F. J. and Abruña, H., *J. Am. Chem. Soc*., **2004**, 126, 4043 – 4049.
25. Dreesen, L.; Humbert, C.; Hollander, P.; Mani, A. A.; Ataka, K.; Thiry, P. A. and Peremans, A., *Chemical Physics Letters*, **2001**, 333, 327 - 331.
26. Lutz, H. Bonding and structure of water molecules in solid hydrates. Correlation of spectroscopic and structural data. In *Solid Materials*; Springer Berlin / Heidelberg, 1988; Vol. 69; pp 97.
27. Stanek, T. and Pytasz, G., *Acta Physica Polonica* **1977**, *A52*, 119.
28. Lai, S. C. S and Koper, M. T. M., *Phys. Chem. Chem. Phys*., **2009**, 11, 10446 – 10456
29. Schmidt, T. J.; Ross, P. N. and Marković, N. M., *J. Phys. Chem. B*, **2001**, 105, 12082 – 12086.

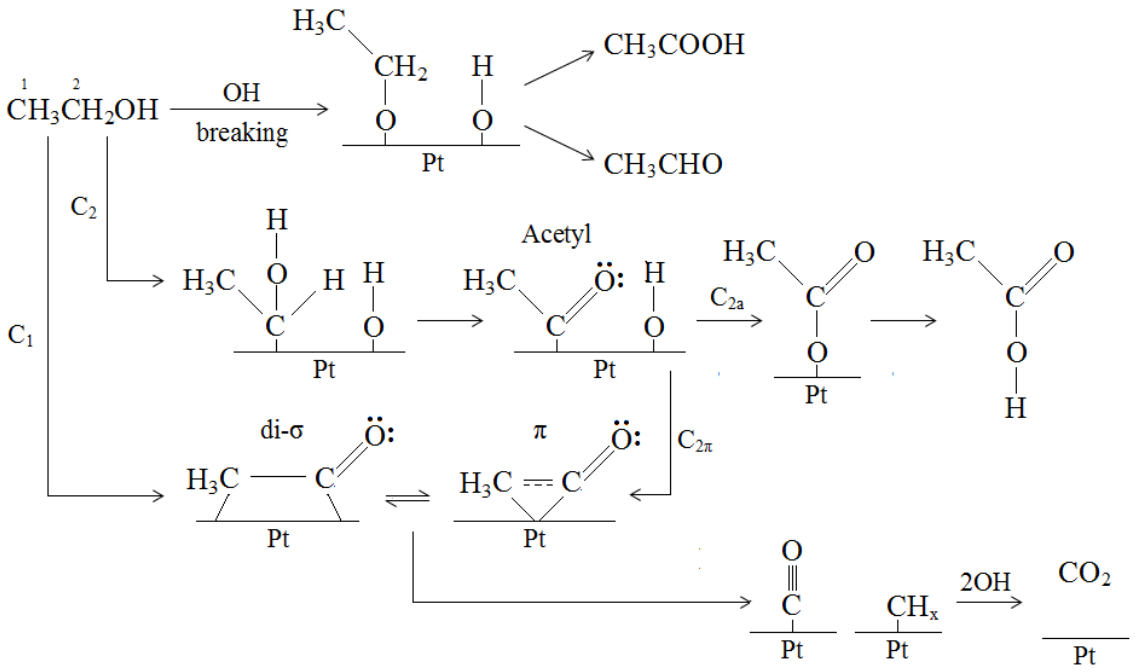

Scheme 1. The mechanism proposed by He et al. for the oxidation of ethanol at Pt. Redrawn from [8].

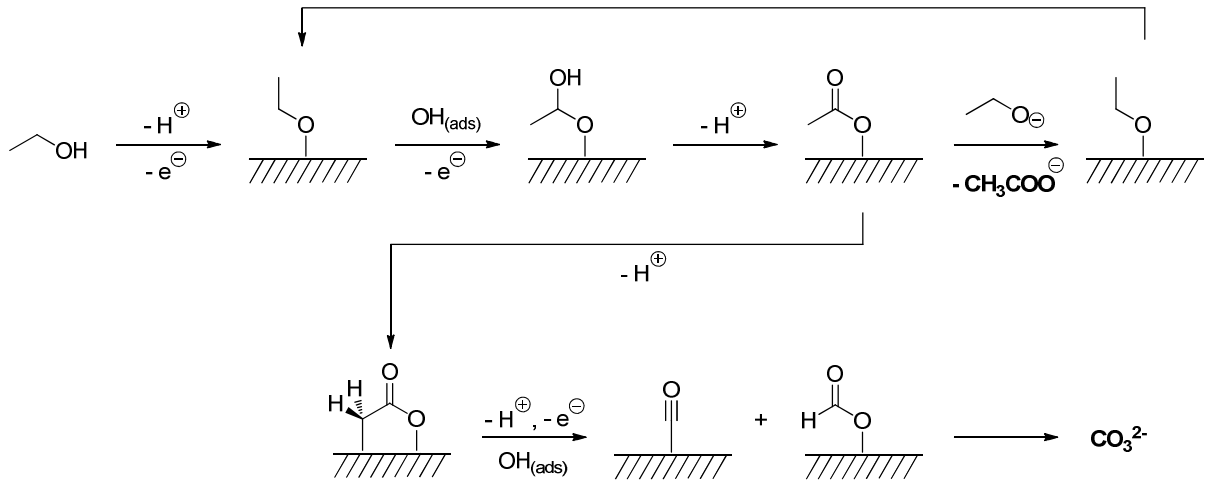

Scheme 2. The mechanism of ethanol oxidation at polycrystalline Pt in alkaline solution proposed by Christensen et al[11].

FIGURE CAPTIONS

Figure 1. Cyclic voltammograms of the Pt electrode in (a) 0.25M KOH and (b) 0.25M KOH + 1M EtOH, in the (i) absence and (ii) presence of an irreversibly-adsorbed Pb layer, scan rate 100 mV s^{-1}.

Figure 2. (i) The current/time profile observed during the FTIR experiment in figure 3, compared to (ii) that observed without Pb.

Figure 3. (a) Spectra (8 cm^{-1} resolution, 100 scans, 47 s per scan set) collected at (i) 0.10, (ii) 0.10 (2 mins), (iii) 0.15, (iv) 0.25, (v) 0.35, (vi) 0.45, (vii) 0.55V during an experiment in which the potential of the polycrystalline Pt electrode was held at 0.15V vs. RHE in N_2-saturated 0.25 M KOH, Pb(IV) acetate added to a concentration of 1 mM and then diluted to < 0.004 mM, ethanol added to a final concentration of 1 M, and the electrode pushed against the CaF_2 prism window and the potential stepped up to 0.20V and then 1.35V in 100 mV increments. The spectra are normalized to that collected at 0.1 V. (b) Spectrum collected at 0.25V in fig. 3(a) from 2000-1150 cm^{-1}. (c) Spectra collected at (i) 0.55, (ii) 0.65, (iii) 0.75 and (iv) 0.85V during the experiment depicted in (a).

Figure 4. The spectrum of (i) aqueous carbonate compared to (ii) that collected at 0.45V in fig. 3(a). See text for details.

Figure 5. Plots of the band intensities of the features in fig. 3 and in an analogous experiment in the absence of Pb (see figs. 7 and 8): (i) CO_3^{2-} Pb/Pt, (ii) 1554 cm^{-1} Pb/Pt, (iii) 1554 cm^{-1} Pt, (iv) 3680 Pt-OH and (v) CO_B x 1000.

Figure 6. The spectra collected at 0.55V to 0.85V after subtracting the underlying carbonate absorption at 1395 cm^{-1}. The spectrum collected at 0.45V was multiplied by 1.58, 2.18 and 2 and the resulting spectra subtracted from those collected at (i) 0.65V, (ii) 0.75V and (iii) 0.85V, respectively.

Figure 7. The spectra collected at (i) 0.95V to (v) 1.35V in the experiment depicted in fig. 2(a) showing the Pt-OH spectral region.

Figure 8. Spectra (100 co-added and averaged scans at 8 cm^{-1} resolution, *ca*. 35 s per scanset) collected at (i) 0.75V, (ii) 0.85V, (iii) 0.95V and (iv) 1.05V from a polycrystalline Pt electrode immersed in 0.25M KOH and 0.5M sodium acetate during an experiment in which the potential was held at 0.1V, the reference spectrum collected, a second spectrum taken at the same potential, and

then the potential stepped to 0.15V, and increased in 100 mV increments, with further spectra collected at each step.

Figure 9. Spectra (100 co-added and averaged scans at 8 cm^{-1} resolution, *ca*. 35 s per scanset) collected at (i) 0.10V, (ii) 0.15V, (iii) 0.25V, (iv) 0.35V and (v) 0.45V from a polycrystalline Pt electrode immersed in 0.10M KOH and 1.0M ethanol during an experiment in which the potential was held at 0.1V, the reference spectrum collected, a second spectrum taken at the same potential, and then the potential stepped to 0.15V, and increased in 100 mV increments, with further spectra collected at each step.

Figure 10. Repeat of the experiment in fig. 9, except the electrolyte was 0.25M KOH. (i) 0.10V, (ii) 0.15V, (iii) 0.25V and (iv) 0.35V. Current/time profile shown in fig. 2(ii).

Figure 11. Spectra collected at 0.10 V vs. RHE after (i) 1 and (ii) 2 minutes during the experiment depicted in fig. 3.

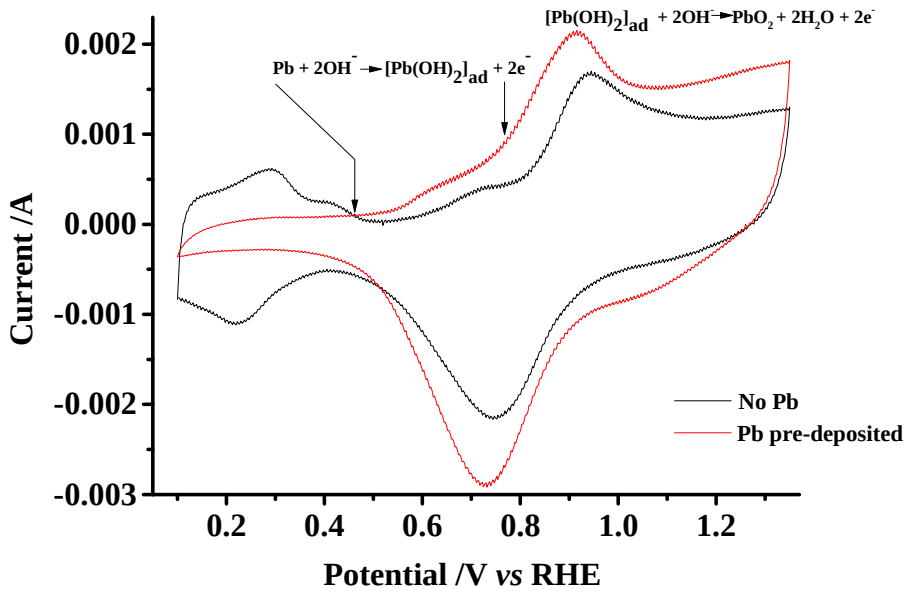
[Pb(OH)2]ad + 2OH- → PbO2 + 2H2O + 2e-
Pb + 2OH- → [Pb(OH)2]ad + 2e-
Current /A
0.002
0.001
0.000
-0.001
-0.002
-0.003
0.2
0.4
0.6
0.8
1.0
1.2
Potential /V vs RHE
No Pb
Pb pre-deposited

(a)

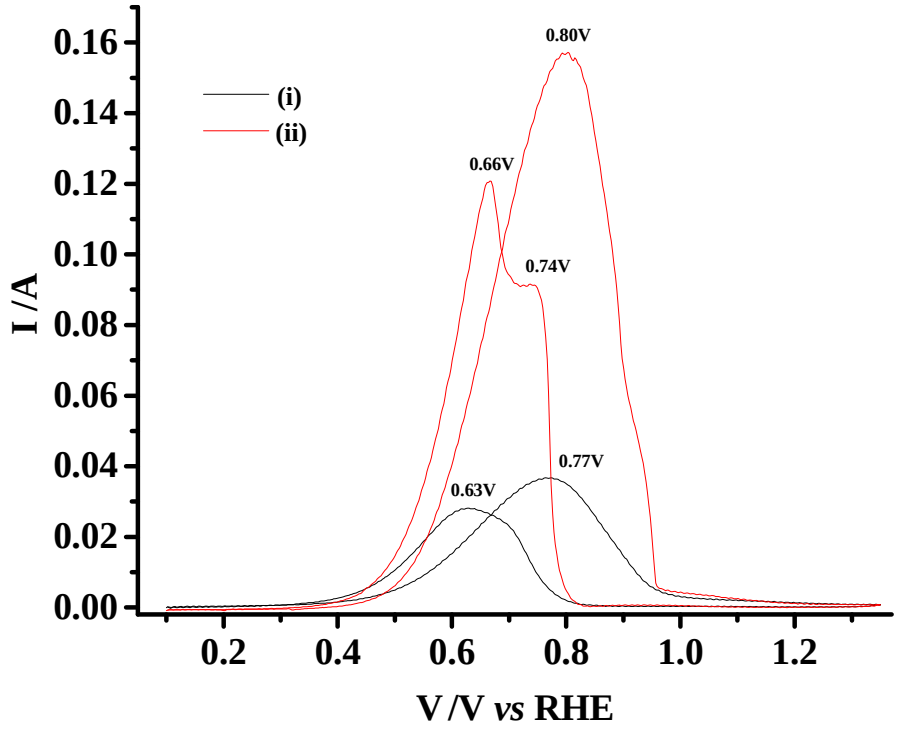
0.80V
(i)
(ii)
0.66V
0.74V
0.77V
0.63V
I /A
0.16
0.14
0.12
0.10
0.08
0.06
0.04
0.02
0.00
0.2
0.4
0.6
0.8
1.0
1.2
V /V vs RHE

(b)

Figure 1

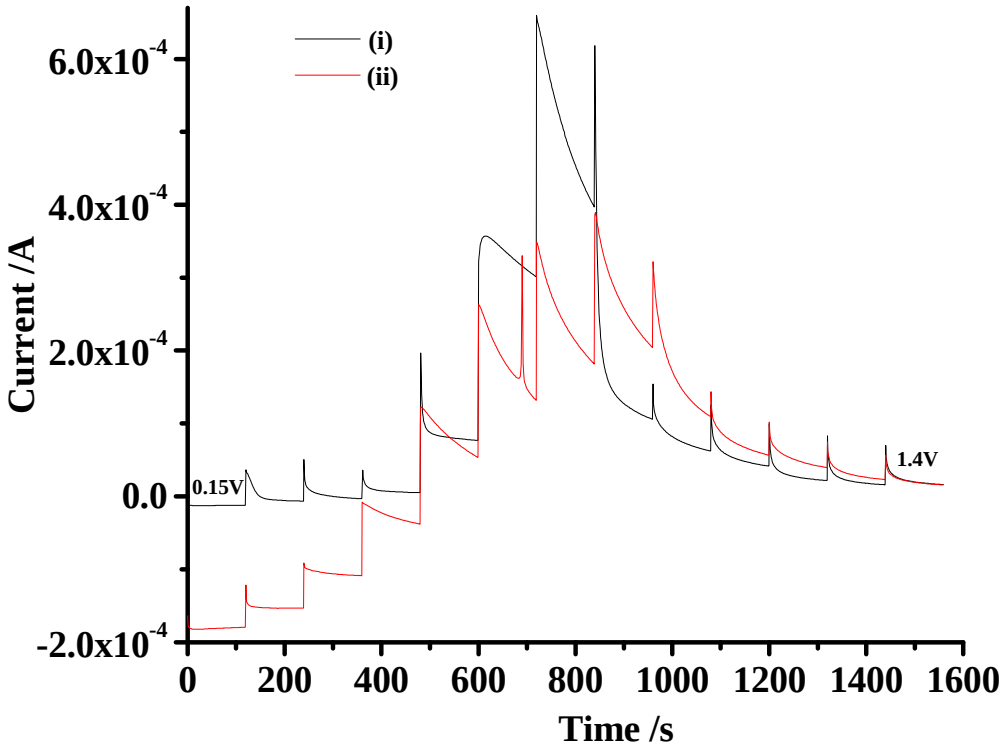

Figure 2

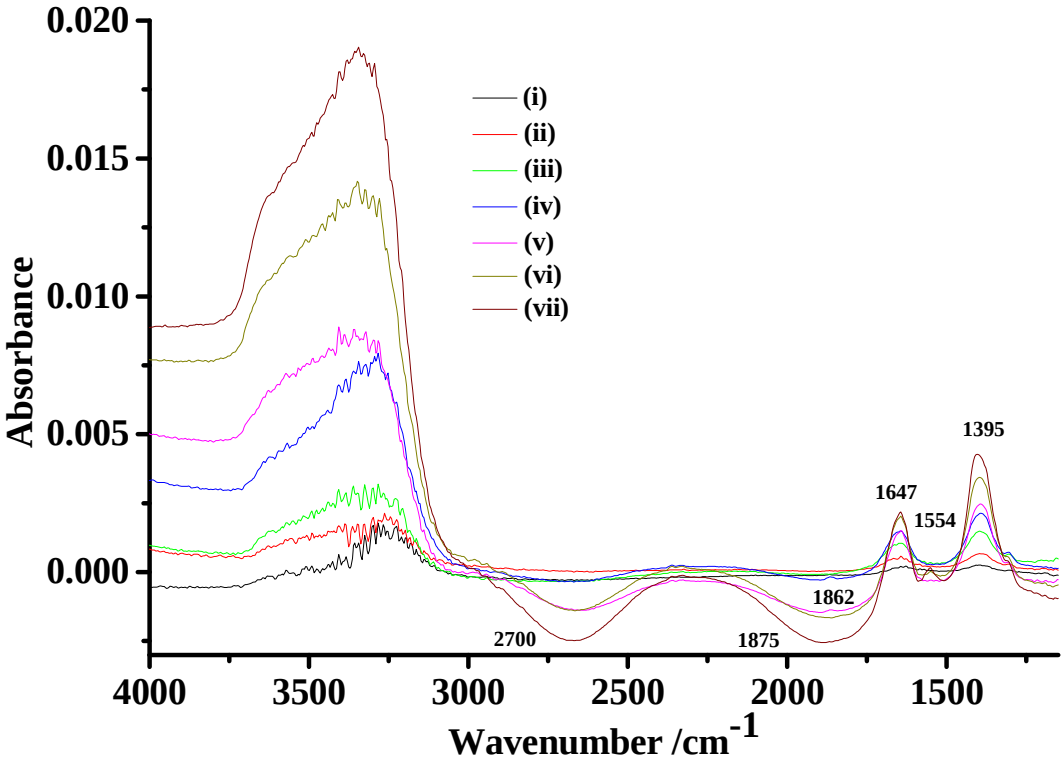

Figure 3(a)

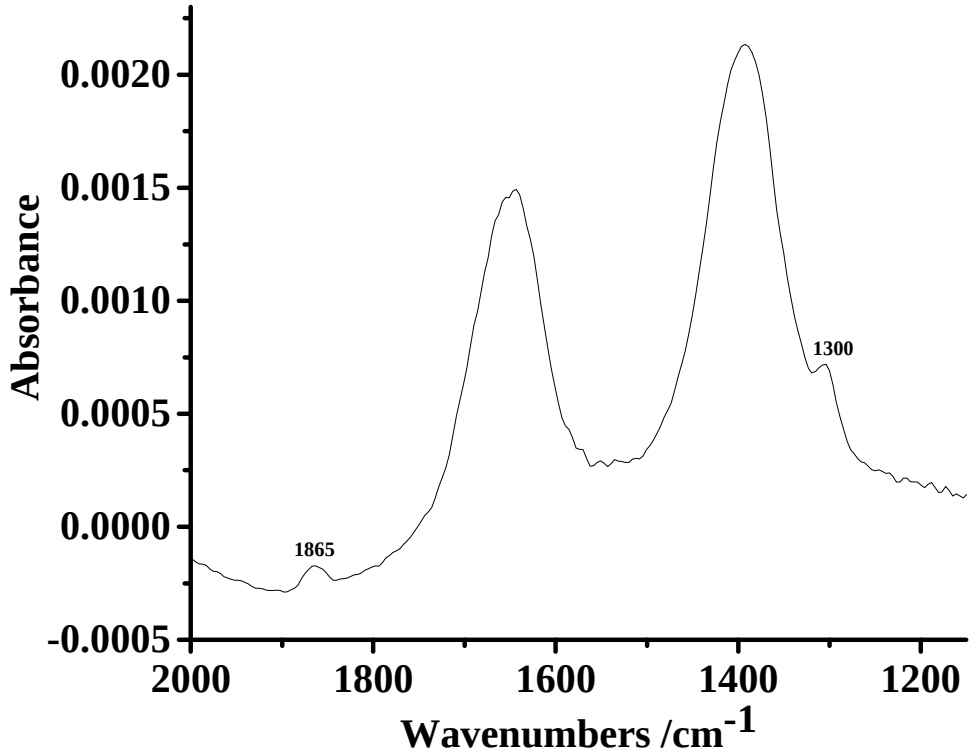

Figure 3(b)

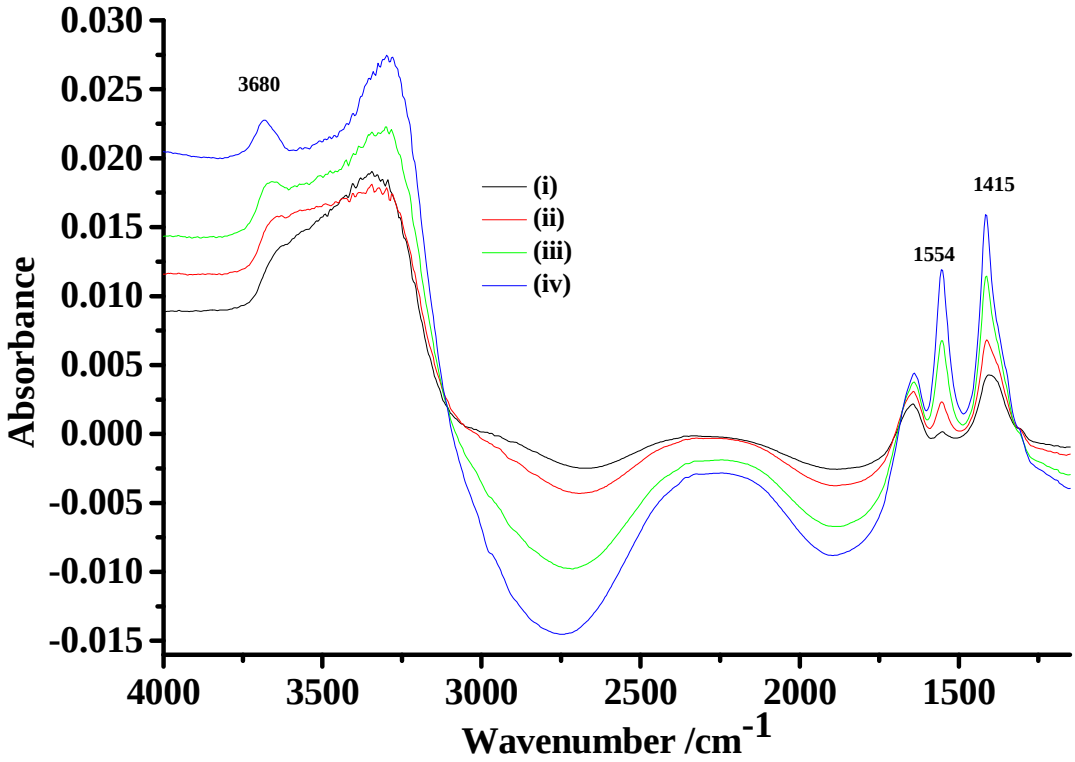

Figure 3(c)

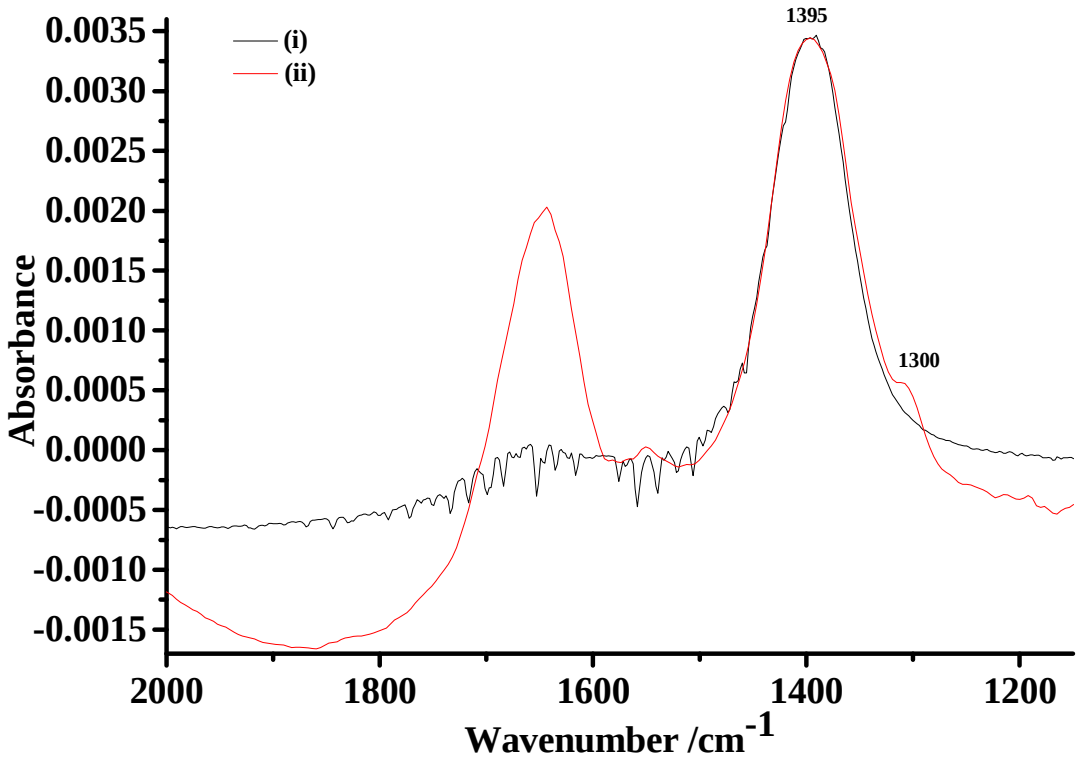

Figure 4

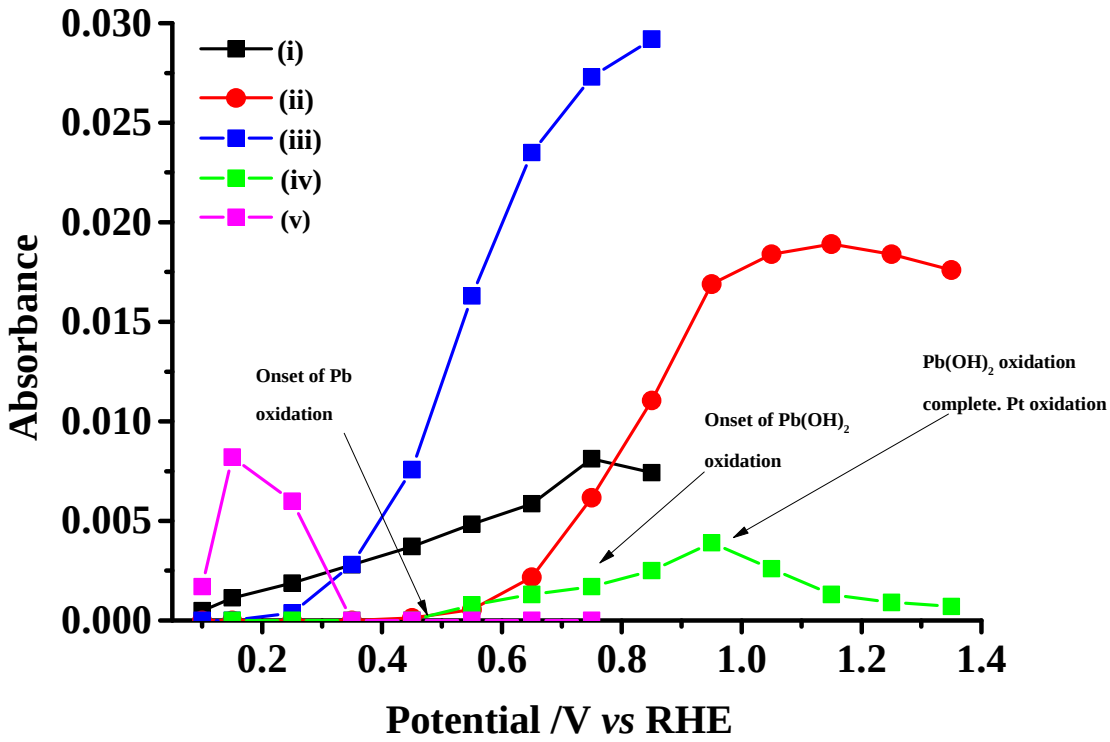

Figure 5

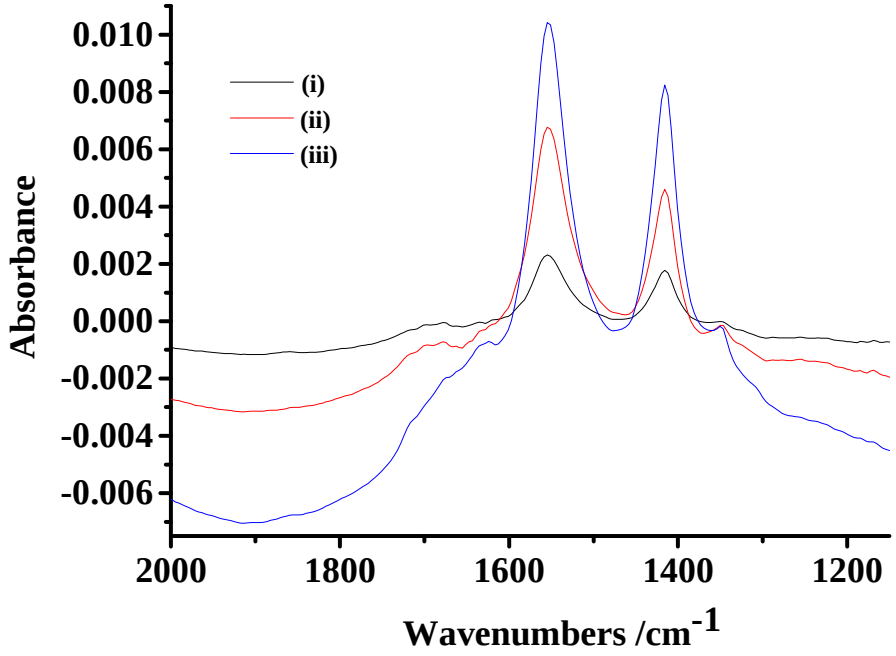

Figure 6

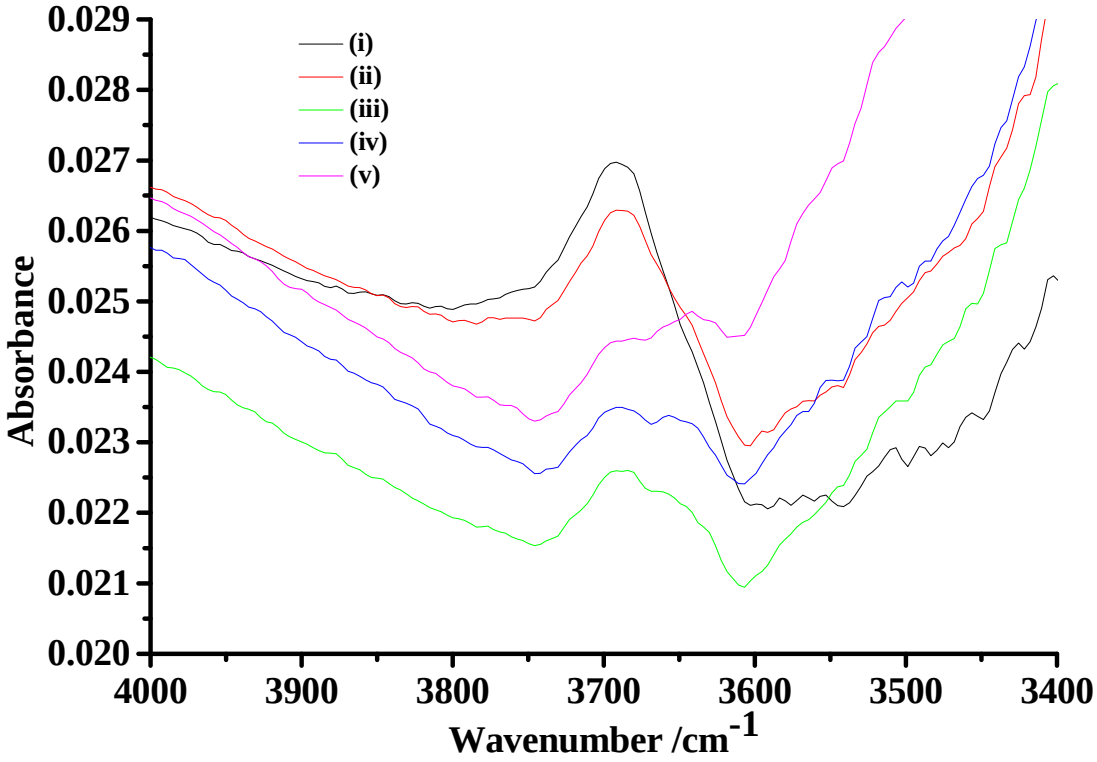

Figure 7

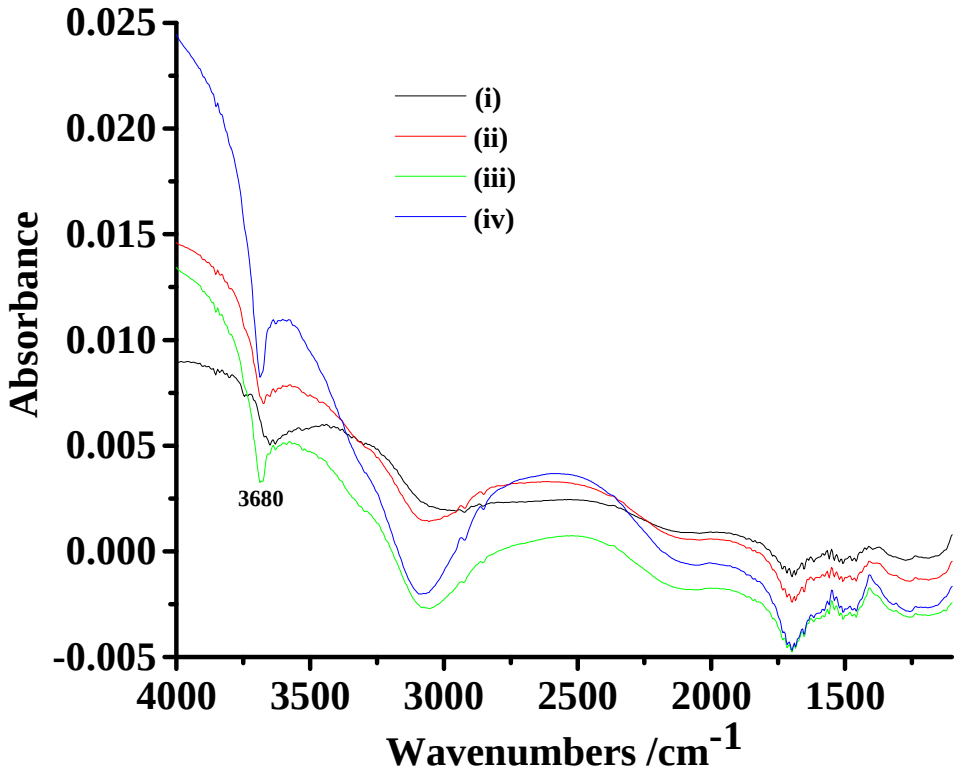

Figure 8

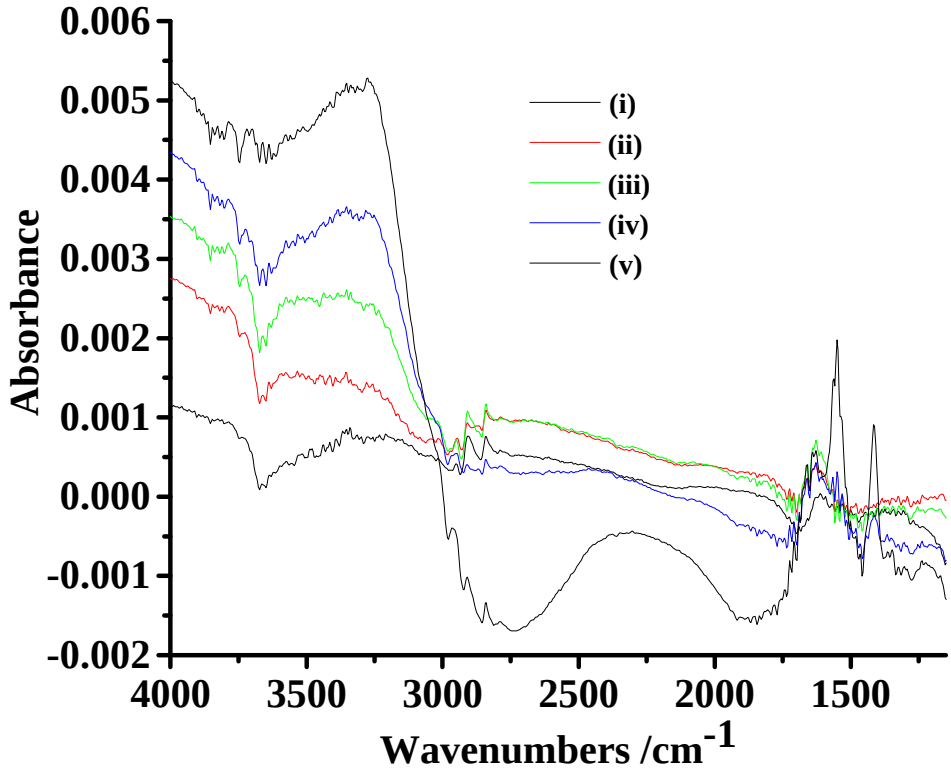

Figure 9

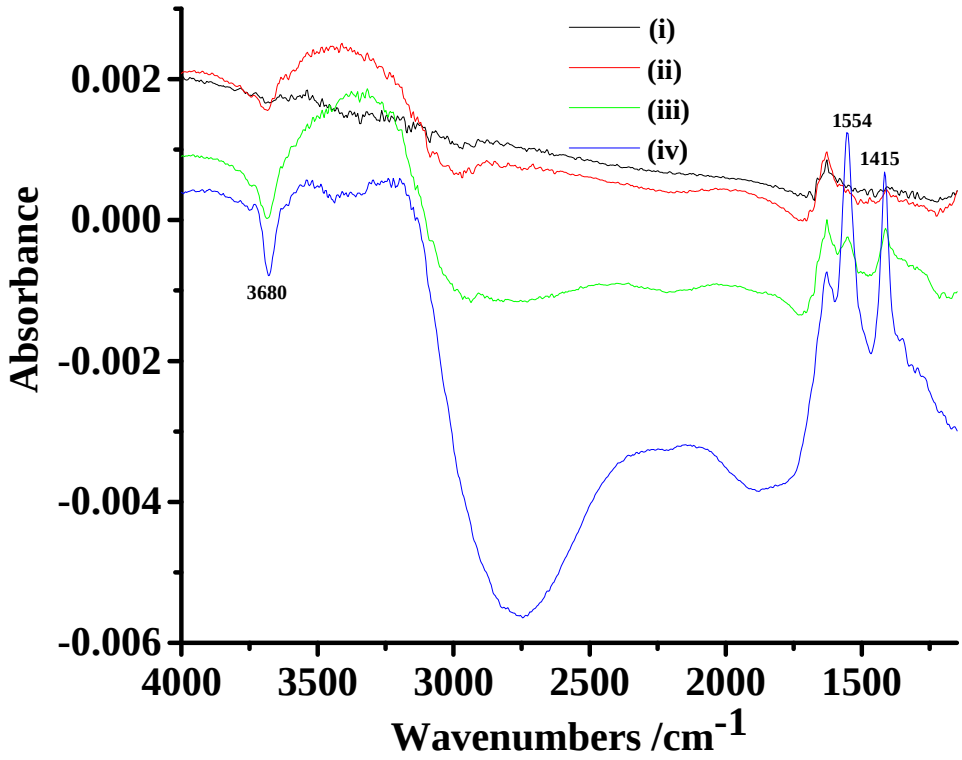

Figure 10

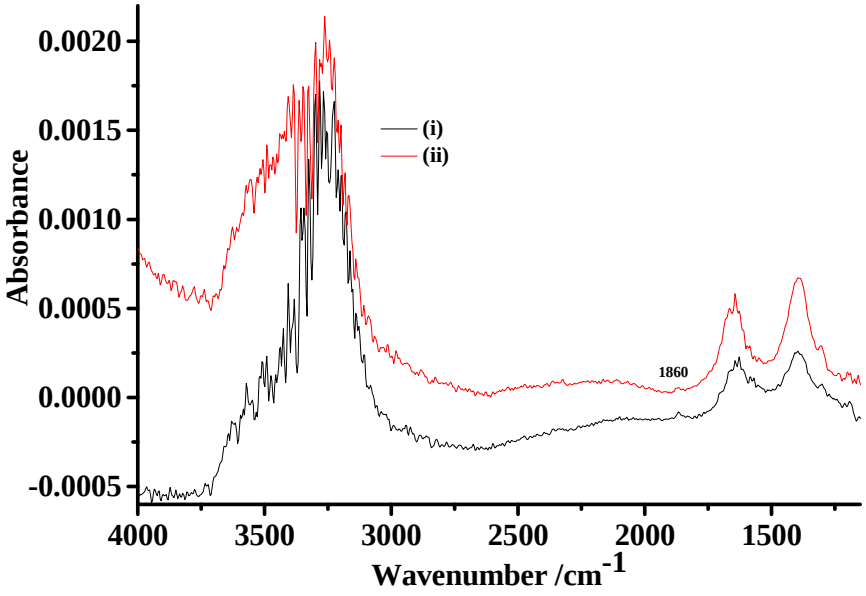

Figure 11